山形大学紀要（工学）第12巻 第1号 昭和47年1月
Bull. of Yamagata Univ. Eng., Vol. 12 No.1 Jan. 1972

# On The Vibration of A Combined Cylindrical Shell (Displacement, Bending Moment and Shearing Force)

Katsuyoshi SUZUKI, Shin TAKAHASHI and
Yoshitarô HIRANO

Department of Mechanical Engineering, Faculty of Engineering

**Abstract**

The radial displacement, the bending moment and the shearing force are studied in the vibration of a combined cylindrical shell. The combined cylindrical shell consists of two cylindrical shells combined lengthwise, of which the radii are equal to each other while the thicknesses are different. The result is shown in graphs and compared with values of the uniform cylindrical shell.

## 1. Introduction

The vibrations of a cylindrical shell have been studied by Warburton[1],[2] and others. The frequencies of a combined cylindrical shell are also obtained by Warburton and Al-Najafi[3], and the authors[4].

In this paper, the radial displacement, the bending moment and the shearing force of a vibrating combined cylindrical shell are studied as a sequel of the previous research. The combined cylindrical shell consists of two cylindrical shells which are combined longitudinally. The radius of one cylindrical shell is identical with the other while the thickness is different. The boundary conditions considered are (1) to be built-in at both ends of the combined cylindrical shell and (2) to be built-in at one end of the thicker part and free at the other.

In the numerical calculation, the case that the number of waves along circumference is 3, is treated. The radial displacement, the bending moment and the shearing force on a combined cylindrical shell are shown in graphs

and are also compared with those of a cylindrical shell with uniform thickness. In this uniform cylindrical shell, the frequency is equal to that of the combined cylindrical shell and the thickness is identical with thicker one.

From the comparison mentioned above, it is found that there are a little differences in the displacement, moment and force between the combined and the uniform cylindrical shells.

## 2. Nomenclature

We distinguish the two cylindrical shells by suffixes 1 and 2.

$\theta$, $x'$, $z'$ : angular, axial and radial coordinates
The origins are taken at the center of each shell (see Fig. 1)

$R$, $x$ : mean radius of the shells, $x=x'/R$

$2l_1$, $2l_2$ : lengths of the shells

$h_1$, $h_2$ : thicknesses of the shells

$D_1$, $D_2$ : bending rigidities of the plates

$1-\zeta_1$, $1-\zeta_2$ : Poisson's ratios

$\gamma$, $g$, $p$ : specific weight, acceleration of gravity and circular frequency

$\beta$, $\mu$, $\alpha_4$ : $\beta_m = 12R^2/h_m^2$, $\mu_m = l_m/R$, $\alpha_m^4 = \gamma h_m p^2 R^4/gD_m$ $(m = 1, 2)$

$\kappa$, $\lambda$, $\varepsilon$ : $\kappa = D_1/D_2$, $\lambda = h_1/h_2$, $\varepsilon = \mu_2/\mu_1$

$u$, $v$, $w$ : axial, tangential and radial components of displacement

$2n$ : number of nodal generators

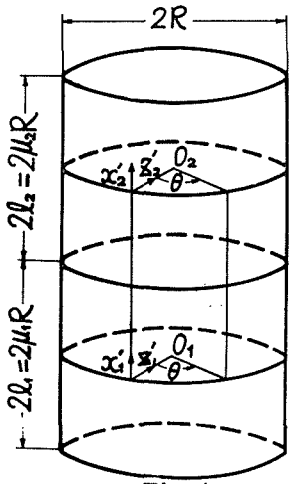


Fig. 1

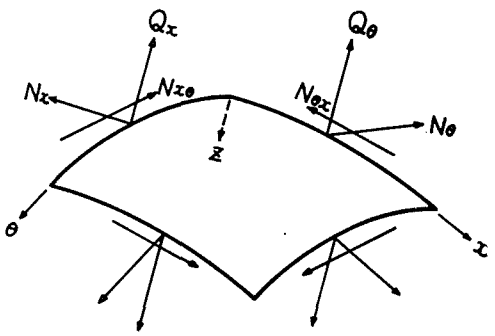


Fig. 2

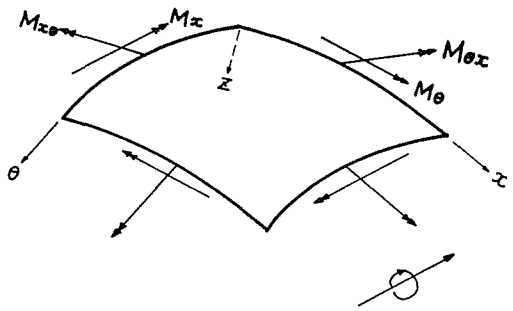


Fig. 3
The positive directions of the moments are shown in the figure.

### 3. Displacement, Moment, Shearing force

The moments and the forces acting on the element of the cylindrical shell are shown in Figs. 2 and 3. The moments $M_x$, $M_{x\theta}$, the shearing force $Q_x$ and the resultant shearing force $V$ are given as follows[5].

$$\left.\begin{aligned} M_x &= -\frac{D}{R^2}\left\{\frac{\partial^2 w}{\partial x^2}+(1-\zeta)\left(\frac{\partial^2 w}{\partial \theta^2}+\frac{\partial v}{\partial \theta}\right)\right\} \\ M_{x\theta} &= -M_{\theta x}=\frac{D\zeta}{R^2}\left(\frac{\partial^2 w}{\partial x\,\partial \theta}+\frac{\partial v}{\partial x}\right) \\ Q_x &= \frac{1}{R}\left(\frac{\partial M_{\theta x}}{\partial \theta}+\frac{\partial M_x}{\partial x}\right)=-\frac{D}{R^3}\left(\frac{\partial^3 w}{\partial x^3}+\frac{\partial^3 w}{\partial \theta^2\,\partial x}+\frac{\partial^2 v}{\partial \theta\,\partial x}\right) \\ V &= Q_x-\frac{1}{R}\frac{\partial M_{x\theta}}{\partial \theta}=-\frac{D}{R^3}\left\{\frac{\partial^3 w}{\partial x^3}+(1+\zeta)\left(\frac{\partial^3 w}{\partial x\,\partial \theta^2}+\frac{\partial^2 v}{\partial x\,\partial \theta}\right)\right\} \end{aligned}\right\} \quad \cdots\cdots(1)$$

The Lagrangian L of a cylindrical shell in a period of its vibration is given from Reference (6) as follows.

$$\begin{aligned} -L=\frac{D}{2R^2}\int_{-\pi}^{\pi}\Bigg[ & -\left\{\frac{\partial^3 w}{\partial x^3}+(1+\zeta)\left(\frac{\partial^3 w}{\partial x\,\partial \theta^2}+\frac{\partial^2 v}{\partial x\,\partial \theta}\right)\right\}w \\ & +\left\{\frac{\partial^2 w}{\partial x^2}+(1-\zeta)\left(\frac{\partial^2 w}{\partial \theta^2}+\frac{\partial v}{\partial \theta}\right)\right\}\frac{\partial w}{\partial x} \\ & +\beta\left\{\frac{\partial u}{\partial x}+(1-\zeta)\left(\frac{\partial v}{\partial \theta}-w\right)\right\}u \\ & +\left\{\frac{\beta\zeta}{2}\left(\frac{\partial v}{\partial x}+\frac{\partial u}{\partial \theta}\right)+2\zeta\left(\frac{\partial^2 w}{\partial x\,\partial \theta}+\frac{\partial v}{\partial x}\right)\right\}v\Bigg]\Bigg|_{x=-\mu}^{x=\mu} d\theta \end{aligned} \quad \cdots\cdots(2)$$

The first term of the right-hand side in Eq. (2) consists of the product of the resultant shearing force $V$ and the displacement $w$ and the second term the product of the bending moment $M_x$ and the angular displacement $\frac{\partial w}{\partial x}$. The third term consists of the product of the normal force and the displace-

ment and the fourth term the product of the resultant tangential force and the displacement respectively.

In the vibration of a cylindrical shell, the stress due to bending moment is eminent in comparison with others. We consider the resultant shearing force $V$ and the bending moment $M_x$ in this paper. Index $m$ ($m=1$ or 2) is introduced to distinguish the two cylindrical shells.

The displacements $u_m$, $v_m$ and $w_m$ are expressed as follows (see Appendix).

$$\begin{aligned} u_m &= \sum_{n=1}^{\infty}\sum_{p=1}^{4} \phi_{nmp}\,(k_{nmp}\ cosh\lambda_{nmp}x_m + k'_{nmp}\ sinh\lambda_{nmp}x_m)\ \cos n\theta \\ -v_m &= \sum_{n=1}^{\infty}\sum_{p=1}^{4} \psi_{nmp}\,(k_{nmp}\ sinh\lambda_{nmp}x_m + k'_{nmp}\ cosh\lambda_{nmp}x_m)\ \sin n\theta \\ w_m &= \sum_{n=1}^{\infty}\sum_{p=1}^{4} (k_{nmp}\ sinh\lambda_{nmp}x_m + k'_{nmp}\ cosh\lambda_{nmp}x_m)\cos n\theta \end{aligned} \qquad \cdots\cdots(3)$$

where

$$\left.\begin{aligned} k_{nmp} &= a_{nm}A_{nmp} + c_{nm}C_{nmp} + g_{nm}G_{nmp} + p_{nm}P_{nmp} \\ k'_{nmp} &= a'_{nm}A'_{nmp} + c'_{nm}C'_{nmp} + g'_{nm}G'_{nmp} + p'_{nm}P'_{nmp} \end{aligned}\right\} \qquad \cdots\cdots(4)$$

Substituting $u_m$, $v_m$ and $w_m$ in Eqs. (3) into the terms of the moment $M_x$ and the resultant shearing force $V$ in Eqs. (1), we obtain

$$\begin{aligned} Mx_m = -\frac{D_m}{R^2}\sum_{n=1}^{\infty}\sum_{p=1}^{4} \Big[ \Big\{\lambda_{nmp}^{\ 2} - (1-\zeta_m)(n^2+n\phi_{nmp})\Big\} \\ (k_{nmp}\ sinh\lambda_{nmp}x_m + k'_{nmp}\ cosh\lambda_{nmp}x_m)\Big]\cos n\theta \\ V_m = -\frac{D_m}{R^3}\sum_{n=1}^{\infty}\sum_{p=1}^{4} \Big[ \Big\{\lambda_{nmp}^{\ 3} - (1+\zeta_m)(n^2+n\phi_{nmp})\,\lambda_{nmp}\Big\} \\ (k_{nmp}\ cosh\lambda_{nmp}x_m + k'_{nmp}\ sinh\lambda_{nmv}x_m)\Big]\cos n\theta \end{aligned} \qquad \cdots\cdots(5)$$

For the combined cylindrical shell of which one end is built-in at $x_1=-\mu_1$ and the other free at $x_2=\mu_2$, the stationary conditions are expressed as follows[4].

$$\begin{aligned} &a_{n1}E_{11} + c_{n1}E_{12} + g_{n1}E_{13} + p_{n1}E_{14} + 2a_{n2}a'_{s2} + 2c_{n2}a'_{c2} + 2g_{n2}a'_{g2} + 2p_{n2}a'_{p2} = 0 \\ &a_{n1}E_{12} + c_{n1}E_{22} + g_{n1}E_{23} + p_{n1}E_{24} - 2\varepsilon a_{n2}a'_{c2} - 2\varepsilon c_{n2}c'_{s2} - 2\varepsilon g_{n2}c'_{g2} - 2\varepsilon p_{n2}c'_{p2} = 0 \\ &a_{n1}E_{13} + c_{n1}E_{23} + g_{n1}E_{33} + p_{n1}E_{34} - 2a_{n2}a'_{g2} - 2c_{n2}c'_{g2} - 2g_{n2}g'_{s2} - 2p_{n2}g'_{p2} = 0 \\ &a_{n1}E_{14} + c_{n1}E_{24} + g_{n1}E_{34} + p_{n1}E_{44} + 2a_{n2}a'_{p2} + 2c_{n2}c'_{p2} + 2g_{n2}g'_{p2} + 2p_{n2}p'_{s2} = 0 \\ &2a_{n1}a'_{s2} - 2\varepsilon c_{n1}a'_{c2} - 2g_{n1}a'_{g2} + 2p_{n1}a'_{p2} + a_{n2}a_{s2} + c_{n2}a_{c2} + g_{n2}a_{g2} + p_{n2}a_{p2} = 0 \\ &2a_{n1}a'_{c2} - 2\varepsilon c_{n1}c'_{s2} - 2g_{n1}c'_{g2} + 2p_{n1}c'_{p2} + a_{n2}a_{c2} + c_{n2}c_{s2} + g_{n2}c_{g2} + p_{n2}c_{p2} = 0 \\ &2a_{n1}a'_{g2} - 2\varepsilon c_{n1}c'_{g2} - 2g_{n1}g'_{s2} + 2p_{n1}g'_{p2} + a_{n2}a_{g2} + c_{n2}c_{g2} + g_{n2}g_{s2} + p_{n2}g_{p2} = 0 \\ &2a_{n1}a'_{p2} - 2\varepsilon c_{n1}c'_{p2} - 2g_{n1}g'_{p2} + 2p_{n1}p'_{s2} + a_{n2}a_{p2} + c_{n2}c_{p2} + g_{n2}g_{p2} + p_{n2}p_{s2} = 0 \end{aligned} \qquad (6)$$

where

$$E_{11} = 4a_{s2}' + \kappa a_{s1} \qquad E_{23} = 4\varepsilon c_{g2}' + \kappa c_{g1}$$

$$E_{12} = -4\varepsilon a_{c2}' + \kappa a_{c1} \qquad E_{24} = -4\varepsilon c_{p2}' + \kappa c_{p1}$$

$$E_{13} = -4a_{g2}' + \kappa a_{g1} \qquad E_{33} = 4g_{s2}' + \kappa g_{s1}$$

$$E_{14} = 4a_{p2}' + \kappa a_{p1} \qquad E_{34} = -4g_{p2}' + \kappa g_{p1}$$

$$E_{22} = 4\varepsilon^2 c_{s2}' + \kappa c_{s1} \qquad E_{44} = 4p_{s2}' + \kappa p_{s1}$$

The stationary conditions for the built-in combined cylindricl shell are

$$\begin{aligned}
&a_{n1}(\kappa a_{s1} + a_{s2}) + c_{n1}(\kappa a_{c1} - \varepsilon a_{c2}) + g_{n1}(\kappa a_{g1} - a_{g2}) + p_{n1}(\kappa a_{p1} + a_{p2}) = 0\\
&a_{n1}(\kappa a_{c1} - \varepsilon a_{c2}) + c_{n1}(\kappa c_{s1} + \varepsilon^2 c_{s2}) + g_{n1}(\kappa c_{g1} + \varepsilon c_{g2}) + p_{n1}(\kappa c_{p1} - \varepsilon c_{p2}) = 0\\
&a_{n1}(\kappa a_{g1} - a_{g2}) + c_{n1}(\kappa c_{g1} + \varepsilon c_{g2}) + g_{n1}(\kappa g_{s1} + g_{s2}) + p_{n1}(\kappa g_{p1} - g_{p2}) = 0\\
&a_{n1}(\kappa a_{p1} + a_{p2}) + c_{n1}(\kappa c_{p1} - \varepsilon c_{p2}) + g_{n1}(\kappa g_{p1} - g_{p2}) + p_{n1}(\kappa p_{s1} + p_{s2}) = 0
\end{aligned} \qquad \cdots\cdots(7)$$

The frequency equation is obtained by equating to zero the determinant of the coefficients of $a_{n1}$, $c_{n1}$, etc. in the above equations.

$a_{s1}$, $a_{s2}$, $a_{c1}$, $\cdots\cdots p_{s1}$ and $p_{s2}$ in the above Eqs. (6) and (7) are identical with $a_{s1}$, $a_{s2}$, $a_{c1}$, $\cdots\cdots$ $p_{s1}$ and $p_{s2}$ in Reference (4). By the frequency epuations derived from Eqs. (6) and (7), we obtain the relations between $\sqrt{\frac{\alpha^4}{\beta}}$ and $\mu$ for any $n$, $\kappa$ and $\varepsilon$. When we give some value to one of the boundary values (e. g. $p_{n2}=1$), the other boundary values are determined and the displacements $u_m$, $v_m$ and $w_m$ are obtained from Eqs. (3). The moment $Mx_m$ and the resultant shearing force $V_m$ are also obtained from Eqs. (5).

## 4. Numerical examples

In the numerical calculation, we consider the two combined shells of $\beta=10^6$, $4\times10^6$ (thickness ratio $\lambda=2$) and $\beta=10^4$, $10^6$ ($\lambda=10$), assuming that the two shells of the combined shell are of the same material. And we obtain the displacements, the moments and the resultant shearing forces for $\sqrt{\frac{\alpha_1^4}{\beta_1}}$ $\left(=\sqrt{\frac{\alpha_2^4}{\beta_2}}\right)=0.1,\ 0.3,\ 0.5,\ 0.7$ in the case of $n=3$, $\zeta_1=\zeta_2=0.7$ (Poisson's ratio=0.3) and $\cos n\theta=1$. We decide the fundamental quantities for a given value of $\sqrt{\frac{\alpha_1^4}{\beta_1}}$ (e. g. the roots of the equation of eighth order, the coefficients of the displacements $u_m$, $v_m$ and $w_m$, etc.) and obtain $\mu$ by making use of them and so it is difficult to compare the combined shell with the uniform shell where the lenths are completly equal. We then compare the combined shell with the uniform shell vibrating at the same frequency ( $=\sqrt{\frac{\alpha_1^4}{\beta_1}}$ ) to see the tendency of distribution of displacement, moment and shearing force.

In the beginning, we describe the built-in-free combined cylindrical shell. The solution of the Eqs. (6) is shown in Fig.4 in which we take $\mu_1 + \mu_2$, $\sqrt{\frac{\alpha_1^4}{\beta_1}}\left(=\sqrt{\frac{\alpha_2^4}{\beta_2}}\right)$ and $\frac{\mu_1}{\mu_1+\mu_2}$ for the coordinate axes. In Figs. 5, 6 and 7, the distributions of the radial displacement $w_m$ for the points on the curves in Fig. 4 are indicated. Figure 5 corresponds to length ratio $\varepsilon = 3$, Fig. 6 to $\varepsilon = 1$ and Fig. 7 to $\varepsilon = \frac{1}{3}$ respectively. We decide the boundary values $a_{n1}$, $c_{n1}$, $g_{n1}$, $p_{n1}$, $a_{n2}$, $c_{n2}$ and $g_{n2}$ for $p_{n2} = 1$ from Eqs. (6) and obtain the displacement $w_m$ from Eqs. (3) in the case of $\cos n\theta = 1$ there. In each case, the displacements at the free end are maximum. Discussing the second mode of vibration, in

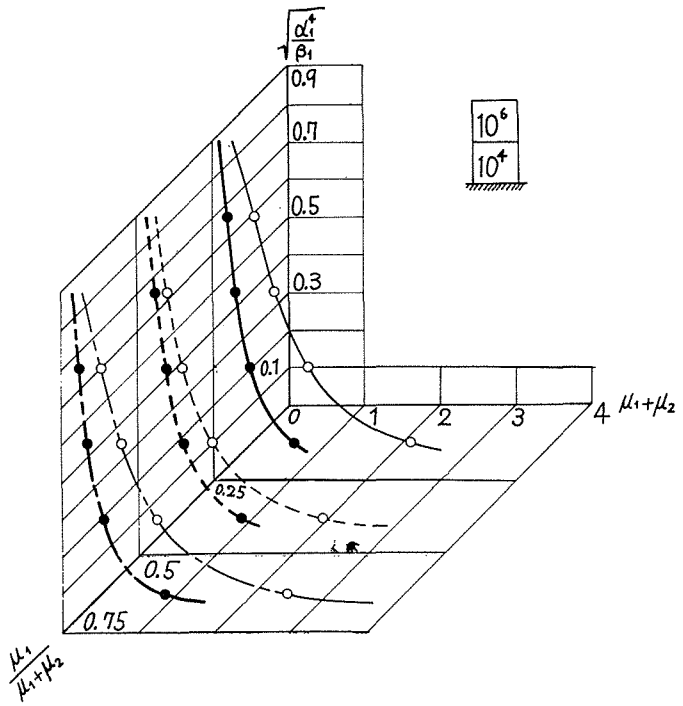


Fig. 4　Frequency curves of the built-in-free combined cylindrical shell (n=3, λ=10)

The frequencies of the combined cylindrical shell of $\beta=10^4$, $10^6$ are shown. The full lines, the broken lines and the chain lines correspond to $\varepsilon = 3$, $1$, $\frac{1}{3}$ respectively. The thick lines indicate the frequency loci for the first mode and the thin lines for the second mode. The open and the solid circles, ○ ● on the curves denote the points of computed displacemet, moment and shearing force.

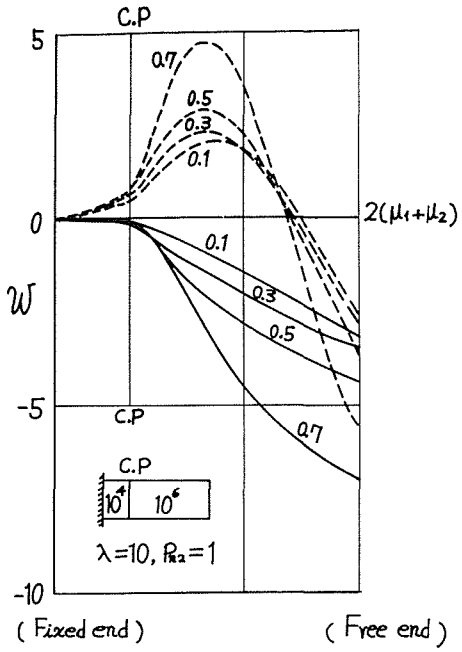


| $\sqrt{\frac{\alpha_1^4}{\beta_1}}$ | $\mu_1$ (first mode) | $\mu_1$ (second mode) |
|---|---|---|
| 0.1 : | 0.2712 | 0.6546 |
| 0.3 : | 0.1252 | 0.3116 |
| 0.5 : | 0.0756 | 0.2019 |
| 0.7 : | 0.0462 | 0.1361 |

Fig. 5 Displacements $w$ of the built-in-free combined cylindrical shell ( $\varepsilon = 3$, $n = 3$ )

The left end of the abscissa axis corresponds to the built-in end and the right end to the free end. The position of the connecting section is denoted by C. P. Integers of the curves denote the values of $\sqrt{\frac{\alpha_1^4}{\beta_1}}$ . The full lines indicate the deflection curves for the first mode and the broken lines for the second mode.

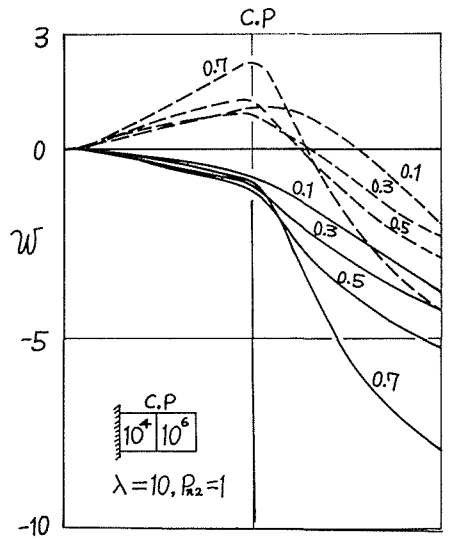


| $\sqrt{\frac{\alpha_1^4}{\beta_1}}$ | $\mu_1$ (first mode) | $\mu_1$ (second mode) |
|---|---|---|
| 0.1 : | 0.6909 | 1.2233 |
| 0.3 : | 0.3157 | 0.4968 |
| 0.5 : | 0.1963 | 0.3074 |
| 0.7 : | 0.1267 | 0.2028 |

Fig. 6 Displacements $w$ of the built-in-free combined cylindrical shell ( $\varepsilon = 1$, $n = 3$ )

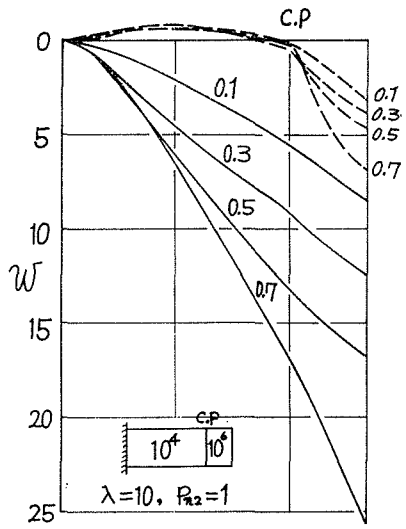


| $\sqrt{\frac{\alpha_1^4}{\beta_1}}$ | $\mu_1$ (first mode) | $\mu_1$ (second mode) |
|---|---|---|
| 0.1 : | 1.0230 | 2.2269 |
| 0.3 : | 0.4065 | 0.9382 |
| 0.5 : | 0.2555 | 0.5983 |
| 0.7 : | 0.1759 | 0.4009 |

Fig. 7　Displacements $w$ of the built-in-free combined cylindrical shell ($\varepsilon = \frac{1}{3}$, n = 3)

the thin part of the shell with free end, the extreme value of the displacements can be seen near the connecting section when $\varepsilon = 1$ and 3 and while, it can be seen in the thick part of the shell when $\varepsilon = \frac{1}{3}$. In the second mode of vibration, there is one nodal circle. And in the case of $\varepsilon = 3$ (Fig. 5), the displacements in the part of the shell of $\beta = 10^4$ are much smaller than those of the shell of $\beta = 10^6$ and the curves of displacements in the part of the shell of $\beta = 10^6$ approximately agree with those of a built-in-free uniform shell of $\beta = 10^6$. In the case of $\varepsilon = \frac{1}{3}$ (Fig. 7), on the contrary, the deflection curves of the part of the shell of $\beta = 10^4$ approximately accord with the ones of a built-in-free uniform shell of $\beta = 10^4$. When we connect the two cylindrical shells of the thickness ratio 1 : 2 and of the same length, the deflection curves which are not shown in graphs are little different from those of a uniform shell of almost the same length as that of the combined shell and of the same thickness as the thick thickness of the combined shell. Figure 8 shows the distributions of the moment and the resultant shearing force along the $x$ axis corresponding to the points (solid circles ● on the thick broken line in Fig.4) on the first frequency curve for the built-in-free combined shell of $\beta = 10^4$, $10^6$ in the case of $\varepsilon$=1. The ordinate of the figure takes $p_{n2} D_1/R^2$ for unit bending moment per unit length in the moment $Mx_m$ ($e.g.\ p_{n2} D_1/R^2 = 1 \frac{kg-cm}{cm}$) and takes $p_{n2} D_1/R^3$ for unit force per unit length in the shearing force $V_m$ respectively.

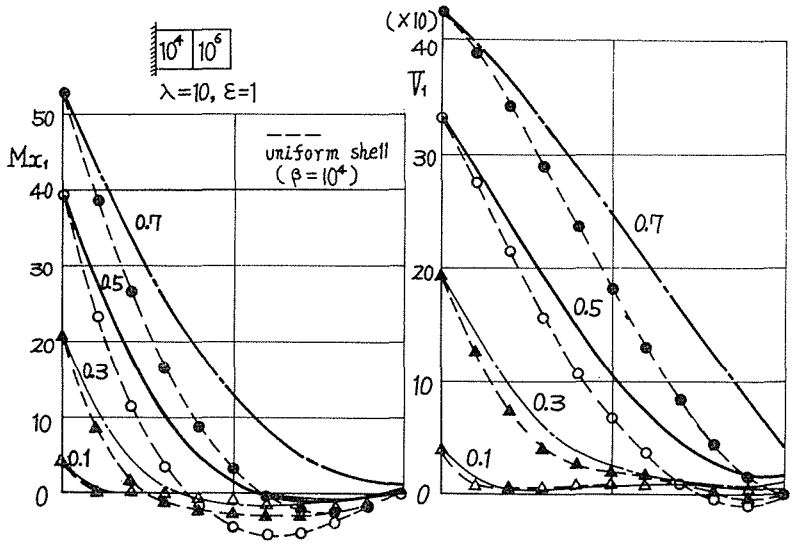


| $\sqrt{\frac{\alpha_1^4}{\beta_1}}$ | $2\mu_1$ (combined shell) | $\mu$ (uniform shell of $\beta = 10^4$) |
|---|---|---|
| 0.1 : | 1.3819 | 1.1361 |
| 0.3 : | 0.6315 | 0.4257 |
| 0.5 : | 0.3926 | 0.2669 |
| 0.7 : | 0.2534 | 0.1840 |

Fig. 8 Distributions of moment and shearing force of the built-in-free combined cylindrical shell (n = 3, first mode)

The distributions of moment and shearing force of the thick part ($\beta = 10^4$) of the combined shell are shown. The left end of the abscissa axis corresponds to the built-in end and the right end to the connecting section. The integers of the curves denote the values of $\sqrt{\frac{\alpha_1^4}{\beta_1}}$. The distributions of moment and shearing force of a built-in-free uniform shell ($\beta = 10^4$) of the same frequency $\sqrt{\frac{\alpha_1^4}{\beta_1}}$ as that of the combined shell are indicated by the broken lines. In this case, the right end of the abscissa axis corresponds to the free end. For convenience sake, their distribution curves are plotted to have the same ordinates for the maximum moments and maximum shearing forces of the combined shell and the uniform shell.

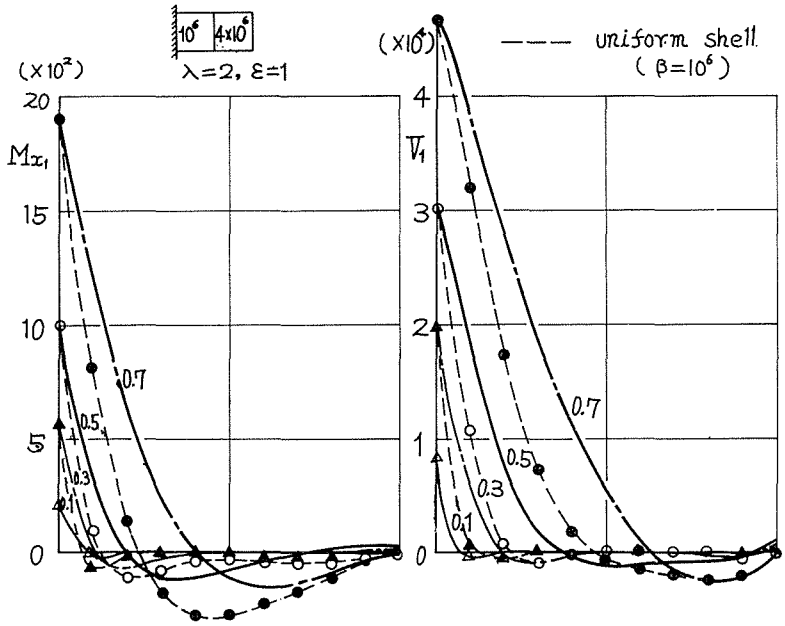


| $\sqrt{\frac{\alpha_1^4}{\beta_1}}$ | $2\mu_1$ (combined shell) | $\mu$ (uniform shell of $\beta = 10^6$) |
|---|---|---|
| 0.1 : | 0.9787 | 0.8483 |
| 0.3 : | 0.4605 | 0.3894 |
| 0.5 : | 0.2792 | 0.2337 |
| 0.7 : | 0.1703 | 0.1422 |

Fig. 9 Distributions of moment and shearing force of the built-in-free combined shell (n = 3, first mode)

The distributions of moment and shearing force of the thick part ($\beta = 10^6$) of the combined shell of $\beta = 10^6$, $4 \times 10^6$ are shown. The distributions of moment and shearing force of a built-in-free uniform shell ($\beta = 10^6$) of the same frequency $\sqrt{\frac{\alpha_1^4}{\beta_1}}$ as that of the combined shell are indicated by the broken lines.

Both of the moment and the resultant shearing force are maximum at built-in end and rapidly become small toward the connecting section. The moment and the shearing force at the connecting section are very small in comparison with those of the built-in end. The moment and the resultant shearing force of the part of the shell of $\beta = 10^6$ are small compared with those of the shell of $\beta = 10^4$ and so, they are omitted in the figure. At the free end, both of the moment and the resultant shearing force

are zero. As shown in Fig. 9, the moment and the resultant shearing force of the combined shell of the thickness ratio $\lambda=2$ are also small at the connecting section. In this case, $p_{n1} D_1/R^2$ is taken to be unit moment per unit length in $Mx_m$ and $p_{n1} D_1/R^3$ to be unit force per unit length in $V_m$. An example similar to this can be seen in Fig. 17. In Figs. 8 and 9, are shown together comparisons in the distributions of the moment and the shearing force between the combined shell and the uniform shell of the same frequency $\sqrt{\frac{\alpha^4}{\beta}}$ as that of the combined shell and of the same thickness as that of the thick part of the shell. In Fig. 8, we compare the combined shell of $\beta = 10^4$, $10^6$ with the built-in-free uniform shell ($\beta = 10^4$) of the same frequency $\sqrt{\frac{\alpha^4}{\beta}}$ as that of the combined shell and of the same thickness as that of the thick part of the shell. The lengths of the combined shell and the uniform shell of $\beta = 10^4$ are shown in the figure and as is evident from it, they are a little different. Figure 9 shows the comparison between the combined shell of

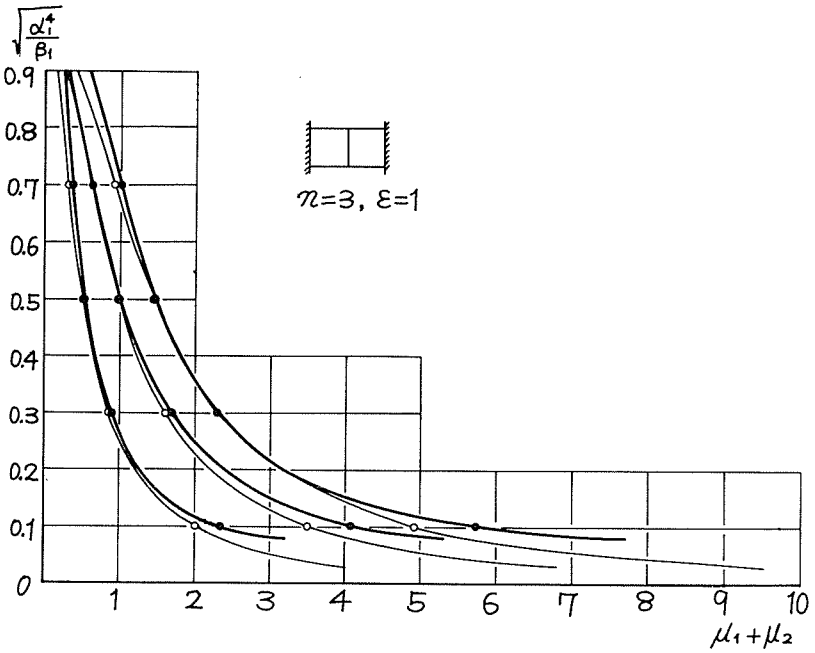


Fig. 10 Frequency curves of the built-in combined shell (first mode ~ third mode)

The frequency curves of the combined shell of equal length ($\mu_1 = \mu_2$) are shown. The thick lines denote the frequency curves of the combined shell of $\beta=10^4$, $10^6$ and the thin lines those of $\beta = 10^6$, $4 \times 10^6$ respectively. The curves correspond to the first, second and third mode of vibration from left to right respectively. The open and the solid circles, ○ ● denote the points of computed displacement, moment and shearing force.

$\beta = 10^6$, $4 \times 10^6$ and the built-in-free uniform shell ($\beta = 10^6$) of the same frequency $\sqrt{\frac{\alpha^4}{\beta}}$ as that of the combined shell. As is evident from the figures, the moment and the shearing force of the built-in-free uniform shell are equal to zero at the right end and except this, the distributions of $Mx$ and $V$ of $\beta = 10^4$ or $\beta = 10^6$ parts of the combined shell are similar to those of the built-in-free uniform shell. And as the combined shell becomes long, $Mx$ and $V$ of $\beta = 10^4$ or $\beta = 10^6$ parts of the shell gradually approach to those of the uniform shell of $\beta = 10^4$ or $\beta = 10^6$. As regards the combined shell, the lengths of the abscissa axes in Figs. 8 and 9 correspond to one-second length of the combined shell (the length of the thick part of the combined shell) and in case of the uniform shell, correspond to the whole length of the shell.

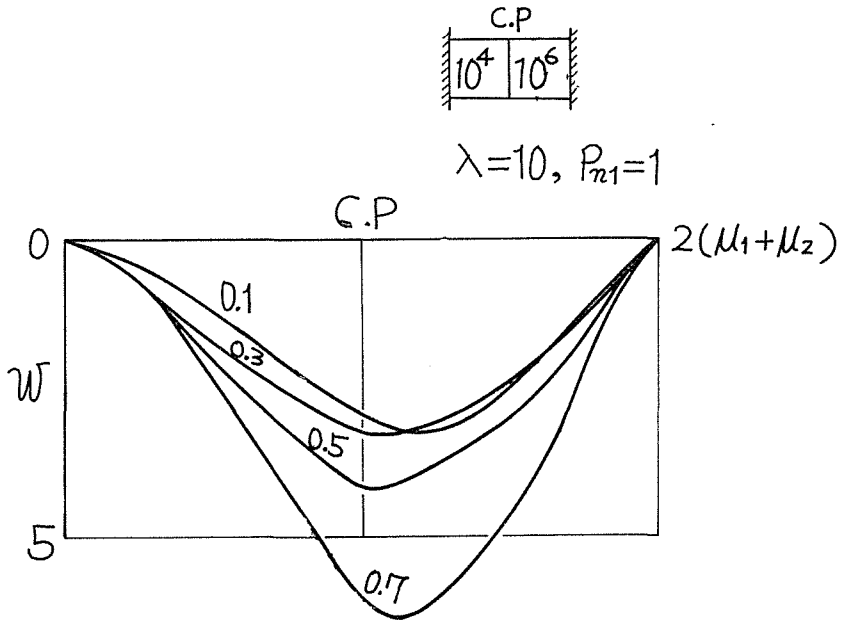


| $\sqrt{\frac{\alpha_1^4}{\beta_1}}$ | $\mu_1$ |
|---|---|
| 0.1 : | 1.1658 |
| 0.3 : | 0.4397 |
| 0.5 : | 0.2710 |
| 0.7 : | 0.1841 |

Fig. 11 Displacements $w$ of the built-in combined shell (n=3, $\varepsilon$=1, first mode)

Both ends of the abscissa axis correspond to the built-in ends. The position of the connecting section is denoted by C. P. The integers of the curves denote the values of $\sqrt{\frac{\alpha_1^4}{\beta_1}}$.

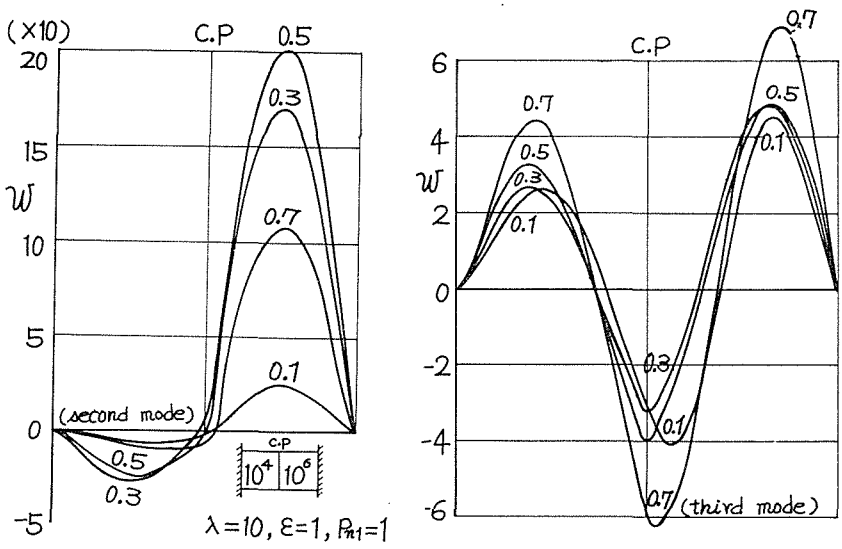


| $\sqrt{\frac{\alpha_1^4}{\beta_1}}$ | $\mu_1$ (second mode) | $\mu_1$ (third mode) |
|---|---|---|
| 0.1 : | 2.0279 | 2.8685 |
| 0.3 : | 0.8489 | 1.1481 |
| 0.5 : | 0.5094 | 0.7278 |
| 0.7 : | 0.3171 | 0.5071 |

Fig. 12 Displacements $w$ of the built-in combined shell (n=3, second and third mode)

Next we describe the built-in combined shell. In this case, we consider only the combined shell with equal length ($\mu_1 = \mu_2$). The solution of the Eqs. (7) is shown in Fig. 10. First, we consider the combined shell of $\beta = 10^4$, $10^6$. The displacements $w$ corresponding to the solid circles ● on the thick full lines in Fig. 10 are shown in Figs. 11 and 12. Figure 11 denotes the deflection curves of the first mode and Fig. 12 those of the second and the third mode. In above calculations of these displacements, the tangential displacement $v$ at the connecting cross section is taken to be unity (i. e., $p_{n1} = 1$). The displacements of the thin part ($\beta = 10^6$) of the combined shell are large compared with those of the thick part ($\beta = 10^4$), especially in the second mode of vibration. The number of nodal circles in the second mode is one and in the third mode is two. In Fig. 13 are shown the distributions of the moment and the resultant shearing force corresponding to the points on the first frequency curves in Fig. 10. The distributions of the moment and the shearing force for the second mode are indicated in Fig. 14. In calculations of $Mx$, we take $p_{n1} D_1/R^2$ to be unit moment per unit length and in calculations of $V$, $P_{n1} D_1/R^3$ to be

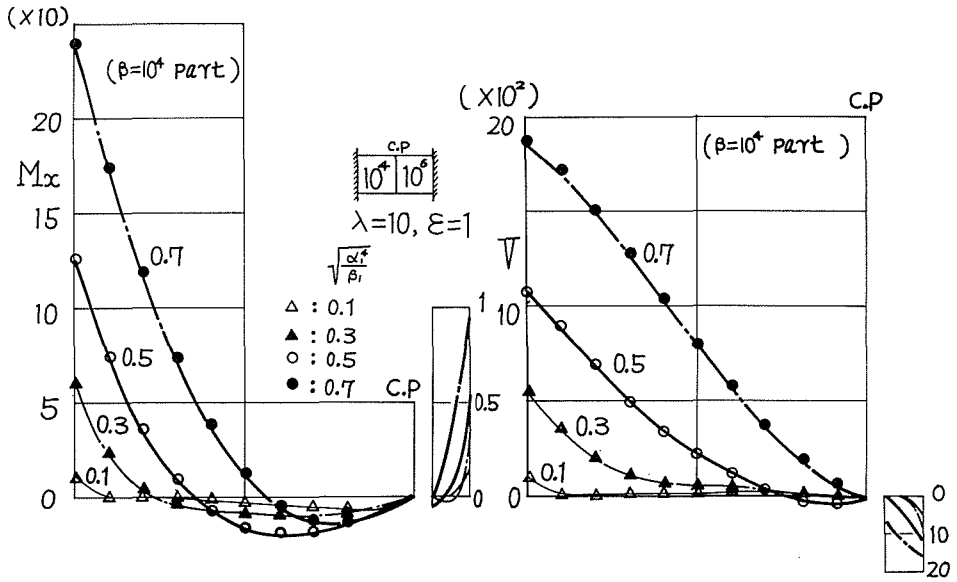


| $\sqrt{\frac{\alpha_1^4}{\beta_1}}$ | $\mu_1$ (combined shell) | $\mu$ (uniform shell of $\beta=10^4$) |
|---|---|---|
| 0.1 : | 1.1658 | 1.1361 |
| 0.3 : | 0.4397 | 0.4257 |
| 0.5 : | 0.2710 | 0.2669 |
| 0.7 : | 0.1841 | 0.1840 |

Fig. 13 Distributions of moment and shearing force of the built-in combined shell (n = 3, first mode)

Both of the moment and the shearing force are maximum at the built-in end of the thick part ($\beta = 10^4$) of the combined shell (at the left end of the abscissa axis) but very small at the connecting section and in the thin part ($\beta = 10^6$). The distributions of the moment and the shearing force in the thin part of $\beta = 10^6$ which are indicated on the right-hand side of each figure are shown only in the range from the clamped end to one-fifth section of the shell. The integers of the curves denote the values of $\sqrt{\frac{\alpha_1^4}{\beta_1}}$. The distributions of moment and shearing force of a built-in-free uniform shell ($\beta=10^4$) of the same frequency $\sqrt{\frac{\alpha_1^4}{\beta_1}}$ as that of the combined shell are indicated by the symbols △, ▲, ○ ●.

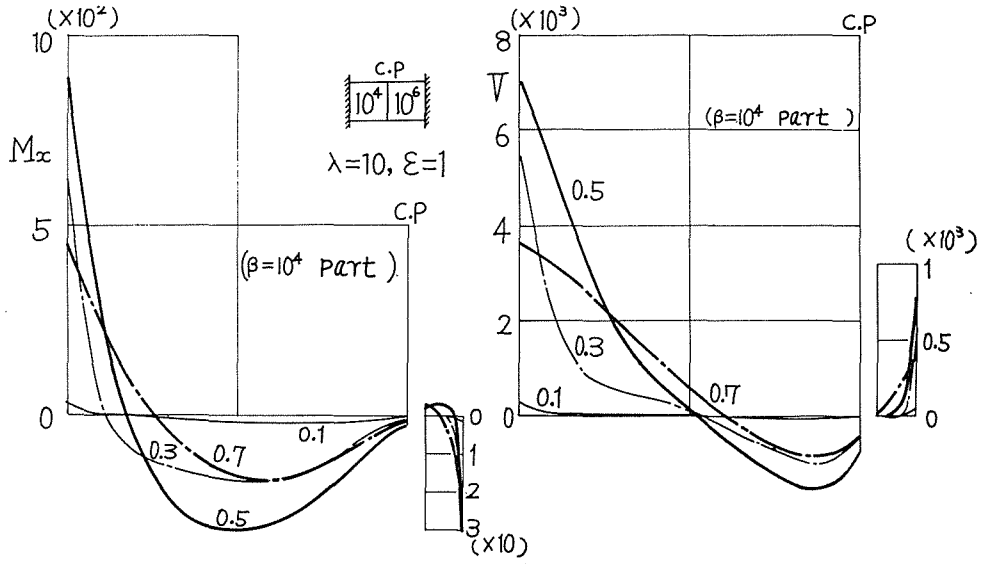


Fig. 14 Distributions of moment and shearing force of the built-in combined shell (n=3, second mode)

unit force per unit length. In addition, the distributions of the moment and the shearing force of the built-in-free uniform shell ($\beta = 10^4$) in the same frequency $\sqrt{\frac{\alpha^4}{\beta}}$ as that of the combined shell are denoted in Fig. 13. The lengths of the two shells shown in the figure are nearly equal. The moments and the resultant shearing forces at the connecting section and in the thin part of $\beta = 10^6$ are small in comparison with those at the clamped end of the thick part of $\beta = 10^4$. With regard to the thin part of $\beta = 10^6$ of the combined shell, only the distributions near the clamped end (from the clamped end to one-fifth section of the shell) are shown. We denote them on the right-hand side of each figure, in which the graduation of the ordinate axis (magnitude of the moment and the sheariug force) is magnified. The distributions of the moment and the shearing force in the thick shell ($\beta = 10^4$) of the combined shell except near the connecting section almost agree with those of the built-in-free uniform shell of $\beta = 10^4$ having about one-second length of the combined shell considered. The right end of the abscissa axis corresponds to the connecting section in the combined shell and to the free end in the uniform shell, respectively. In the uniform shell, both the moment and the shearing force are zero at the free end but not zero at the connecting section of the combined shell.

Next, we shall denote the results of the combined shell connecting two

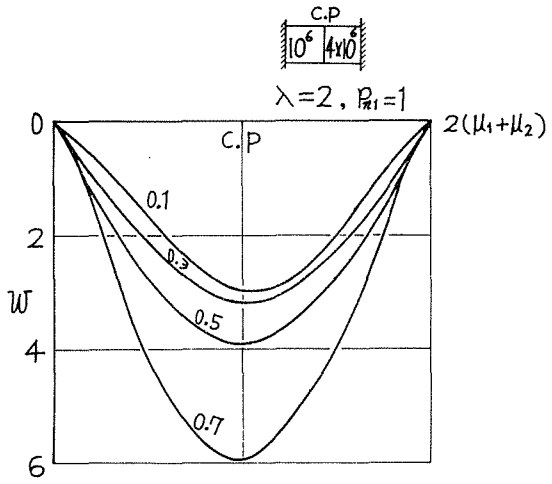


| $\sqrt{\frac{\alpha_1^4}{\beta_1}}$ | $\mu_1$ |
|---|---|
| 0.1 : | 1.0005 |
| 0.3 : | 0.4314 |
| 0.5 : | 0.2523 |
| 0.7 : | 0.1538 |

Fig. 15 Displacements $w$ of the built-in combined shell (n = 3, $\varepsilon = 1$, first mode)

Both ends of the abscissa axis correspond to the built-in ends. The position of the connecting seoction is denoted by C. P. The integers of the curves show the values of $\sqrt{\frac{\alpha_1^4}{\beta_1}}$.

shells of thc thickness ratio 1 : 2 ($\beta = 10^6$, $4 \times 10^6$) in the cases corresponding to the points on the frequency curves shown by the thin lines in Fig. 10. Figure 15 shows the deflection curves of the combined shell of $\beta = 10^6$, $4 \times 10^6$ in the first mode of vibration. Figure 16 denotes the deflection curves in the second and the third mode. The first and the third deflection curves are almost symmetric about the connecting section, while the second deflection curves are almost anti-symmetric. Figure 17 indicates that the moment and the shearing force are maximum at the clamped end in the thick part ($\beta = 10^6$) of the combined shell, but very small at the connecting section and in the thin part ($\beta = 4 \times 10^6$). The distributions of the moment and the shearing force in the thin part of $\beta = 4 \times 10^6$ are indicated only in the range from the clamped end to the one-fifth section of the shell. In Fig. 17 is also made a comparison in the moment and the shearing force between the combined shell and the built-in-free uniform shell ($\beta = 10^6$) vibrating at the same frequency $\sqrt{\frac{\alpha^4}{\beta}}$. For convenience sake, their distribution curves are plotted to have the same ordinates for the maximum moments and the maximum shearing forces of the combined and the uniform shell. As is evident from the figure, the two shells are similar in the distributions of $Mx$ and $V$ except in the neighborhood of the connecting section (and in the neighborhood of the free end of the uniform shell).

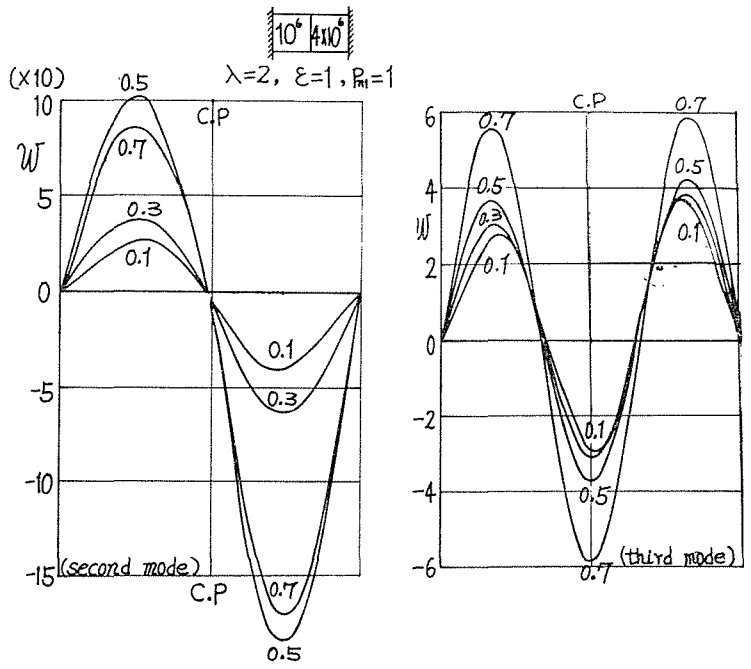


| $\sqrt{\frac{\alpha_1^4}{\beta_1}}$ | $\mu_1$ (second mode) | $\mu_1$ (third mode) |
|---|---|---|
| 0.1 : | 1.7490 | 2.4624 |
| 0.3 : | 0.8012 | 1.1600 |
| 0.5 : | 0.4913 | 0.7236 |
| 0.7 : | 0.3083 | 0.4581 |

Fig. 16 Displacements $w$ of the built-in combined shell (n=3, second and third mode)

When $\sqrt{\frac{\alpha_1^4}{\beta_1}} = 0.7$, the scale of the ordinate for the deflection curve in the second mode of vibration must be multiplied by 10.

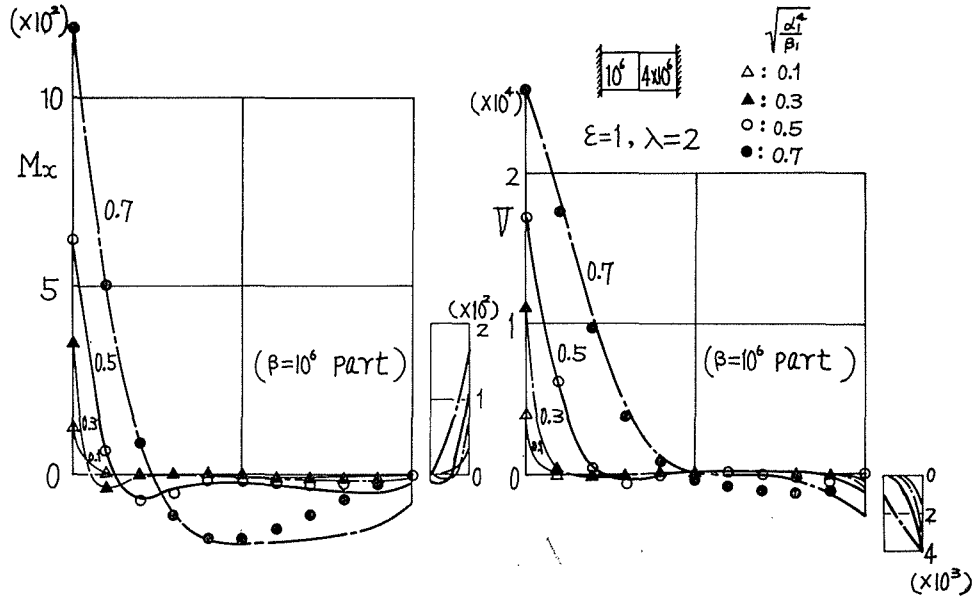


Fig. 17 Distributions of moment and shearing force of the built-in combined shell (n=3, first mode)

Both the moment and the shearing force are maximum at the built-in end of the thick part ($\beta = 10^6$) of the shell (at the left end of the abscissa axis) but very small at the connecting section and in the thin part ($\beta = 4 \times 10^6$). The distributions of moment and shearing force in the thin part of $\beta = 4 \times 10^6$ which are indicated on the right-hand side of each figure are shown only in the range from the clamped end to one-fifth section of the shell. The integers of the curves denote the values of $\sqrt{\frac{\alpha_1^4}{\beta_1}}$. The distributions of moment and shearing force of a built-in-free uniform shell ($\beta = 10^6$) of the same frequency $\sqrt{\frac{\alpha_1^4}{\beta_1}}$ as that of the combined shell are indicated by the symbols △, ▲, ○, ●.

## 6. Conclusion

From the results described above, we may conclude as following. As regards the displacement of the built-in combined shell consisting of the two shells of different thickness, the displacement of the thin part of the combined shell is large as compared with that of the thick part when the thickness ratio is large. But the displacements of both the parts of the combined shell are

almost equal in case of the small thickness ratio.

The deflection curves of the built-in-free combined shell are similar to those of a uniform shell of the same length as that of the combined shell in case of the small thickness ratio. When thickness ratio is large, as the length ratio becomes large, the deflection curves of the long part of the combined shell coincide with those of the uniform shell of the same thickness as that of the long part.

Both the moments and the shearing forces of the built-in-free combined shell and the built-in combined shell are maximum at the built-in ends of the thick parts of the shells. But they are very small at the connecting sections and in the thin parts of the shells. And the distributions of the moment and the shearing force in the thick parts of the shells resemble the ones of the built-in-free uniform shells consisting of only the thick parts of the shells.

The authors wish to express their gratitude to Mr. K. Okazaki and Mrs. T. Yamaguchi of the Faculty of Engineering, Yamagata University for their help in the numerical calculation.

## Appendix

The Euler's equations are given from Reference (6) as follows.

$$\frac{\partial^2 u}{\partial x^2}+\frac{\zeta}{2}\frac{\partial^2 u}{\partial \theta^2}+\frac{\alpha^4}{\beta}u+\left(1-\frac{\zeta}{2}\right)\frac{\partial^2 v}{\partial x\,\partial\theta}-(1-\zeta)\frac{\partial w}{\partial x}=0$$

$$\beta\left(1-\frac{\zeta}{2}\right)\frac{\partial^2 u}{\partial x\,\partial\theta}+\frac{\zeta}{2}(\beta+4)\frac{\partial^2 v}{\partial x^2}+(\beta+1)\frac{\partial^2 v}{\partial\theta^2}+\alpha^4 v+(1+\zeta)\frac{\partial^3 w}{\partial x^2\,\partial\theta}+\frac{\partial^3 w}{\partial\theta^3}-\beta\frac{\partial w}{\partial\theta}=0$$

$$-\beta(1-\zeta)\frac{\partial u}{\partial x}+(1+\zeta)\frac{\partial^3 v}{\partial x^2\partial\theta}+\frac{\partial^3 v}{\partial\theta^3}-\beta\frac{\partial v}{\partial\theta}+\frac{\partial^4 w}{\partial x^4}+2\frac{\partial^4 w}{\partial x^2\partial\theta^2}+\frac{\partial^4 w}{\partial\theta^4}+(\beta-\alpha^4)w=0$$

Equations (3) are the soltions of the Euler's equations. Substituting Eqs. (3) in the Euler's equations, we obtain the following equations.

$$\phi_{nmp}(\lambda_{nmp}^2+a)-\phi_{nmp}\lambda_{nmp}f\zeta_m-\lambda_{nmp}d=0$$

$$2\phi_{nmp}\lambda_{nmp}f+\phi_{nmp}(\lambda_{nmp}^2+b)+2\lambda_{nmp}^2 h-2k=0$$

$$\lambda_{nmp}^4-2n^2\lambda_{nmp}^2+c-\phi_{nmp}\lambda_{nmp}\beta_m d-\phi_{nmp}\beta_m\zeta_m(\lambda_{nmp}^2 h-k)=0$$

where

$$a=-\frac{n^2\zeta_m}{2}+\frac{\alpha_m^4}{\beta_m},\quad b=-\frac{2n^2}{\zeta_m}+\frac{2\alpha_m^4}{\beta_m\zeta_m},\quad c=\beta_m+n^4-\alpha_m^4$$

$$d=1-\zeta_m,\quad f=\frac{n}{\zeta_m}-\frac{n}{2},\quad h=\frac{n(1+\zeta_m)}{\beta_m\zeta_m},\quad k=\frac{n}{\zeta_m}+\frac{n^3}{\beta_m\zeta_m}$$

Eliminating $\phi_{nmp}$ and $\psi_{nmp}$ from these three equations, we obtain

$$\lambda_{nmp}^{8} + \lambda_{nmp}^{6}(a+b-2n^2+2\beta_m\zeta_m h^2+2\zeta_m f^2)$$
$$+ \lambda_{nmp}^{4}[ab+c-2n^2(a+b+2\zeta_m f^2)+2\beta_m\zeta_m(ah^2+2fdh-2hk)-\beta_m d^2]$$
$$+ \lambda_{nmp}^{2}[(a+b)c-2n^2 ab+2\beta_m\zeta_m(k^2-2ahk-2dfk)-\beta_m bd^2+2\zeta_m cf^2]$$
$$+ abc + 2\beta_m\zeta_m ak^2 = 0$$

From the above equations, the quantities $\lambda_{nmp}$, $\phi_{nmp}$ and $\psi_{nmp}$ in Eqs. (3) are obtained.

We assume it possible to expand the values of $u_m$, $v_m$, $w_m$ and $\partial w_m/\partial x_m$ at both ends ($x_m = \pm\mu_m$) of the shells into Fourier series (double signs in the same order), that is,

$$2u_m \Big| x_{m=\pm\mu_m} = \sum_{n=1}^{\infty} (g_{nm} \pm g_{nm}') \cos n\theta$$

$$2v_m \Big| x_{m=\pm\mu_m} = \sum_{n=1}^{\infty} (\mp p_{nm} - p_{nm}') \sin n\theta$$

$$2w_m \Big| x_{m=\pm\mu_m} = \sum_{n=1}^{\infty} (\pm a_{nm} + a_{nm}') \cos n\theta$$

$$2\mu_m \frac{\partial w_m}{\partial x_m} \Big| x_{m=\pm\mu_m} = \sum_{n=1}^{\infty} (c_{nm} \pm c_{nm}') \cos n\theta$$

where the Fourier coefficients $a_{nm}$, $a_{nm}'$, $c_{nm}$, $c_{nm}'$, $g_{nm}$, $g_{nm}'$, $p_{nm}$ and $p_{nm}'$ are the boundary values. Substituting Eqs. (3) in these equations, we obtain

$$k_{nmp} = a_{nm} A_{nmv} + c_{nm} C_{nmv} + g_{nm} G_{nmp} + p_{nm} P_{nmp}$$
$$k_{nmp}' = a_{nm}' A_{nmp}' + c_{nm}' C_{nmp}' + g_{nm}' G_{nmp}' + p_{nm}' P_{nmp}'$$

where $\xi_{nmp} = \lambda_{nmv}\mu_m$

and

$$\Delta_{nm} = (\phi_{nm1}\xi_{nm2} - \phi_{nm2}\xi_{nm1})(\psi_{nm3} - \psi_{nm4}) \cosh\xi_{nm1} \cosh\xi_{nm2} \sinh\xi_{nm3} \sinh\xi_{nm4}$$
$$- (\phi_{nm1}\xi_{nm3} - \phi_{nm3}\xi_{nm1})(\psi_{nm2} - \psi_{nm4}) \cosh\xi_{nm1} \sinh\xi_{nm2} \cosh\xi_{nm3} \sinh\xi_{nm4}$$
$$+ (\phi_{nm1}\xi_{nm4} - \phi_{nm4}\xi_{nm1})(\psi_{nm2} - \psi_{nm3}) \cosh\xi_{nm1} \sinh\xi_{nm2} \sinh\xi_{nm3} \cosh\xi_{nm4}$$
$$+ (\phi_{nm2}\xi_{nm3} - \phi_{nm3}\xi_{nm2})(\psi_{nm1} - \psi_{nm4}) \sinh\xi_{nm1} \cosh\xi_{nm2} \cosh\xi_{nm3} \sinh\xi_{nm4}$$
$$- (\phi_{nm2}\xi_{nm4} - \phi_{nm4}\xi_{nm2})(\psi_{nm1} - \psi_{nm3}) \sinh\xi_{nm1} \cosh\xi_{nm2} \sinh\xi_{nm3} \cosh\xi_{nm4}$$
$$+ (\phi_{nm3}\xi_{nm4} - \phi_{nm4}\xi_{nm3})(\psi_{nm1} - \psi_{nm2}) \sinh\xi_{nm1} \sinh\xi_{nm2} \cosh\xi_{nm3} \cosh\xi_{nm4}$$

$$A_{nmv} = \frac{(-1)^p}{2\Delta_{nm}} [\psi_{nmq}(\phi_{nmr}\xi_{nms} - \phi_{nms}\xi_{nmr}) \sinh\xi_{nmq} \cosh\xi_{nmr} \cosh\xi_{nms}$$
$$+ \psi_{nmr}(\phi_{nms}\xi_{nmq} - \phi_{nmq}\xi_{nms}) \cosh\xi_{nmq} \sinh\xi_{nmr} \cosh\xi_{nms}$$
$$+ \psi_{nms}(\phi_{nmq}\xi_{nmr} - \phi_{nmr}\xi_{nmq}) \cosh\xi_{nmq} \cosh\xi_{nmr} \sinh\xi_{nms}]$$

$$C_{nmp} = \frac{(-1)^p}{2\Delta_{nm}} [\phi_{nmq}(\psi_{nmr}-\psi_{nms})\cosh\xi_{nmq}\sinh_{nmr}\sinh\xi_{nms}$$
$$+ \phi_{nmr}(\psi_{nms}-\psi_{nmq})\sinh\xi_{nmq}\cosh\xi_{nmr}\sinh\xi_{nms}$$
$$+ \phi_{nms}(\psi_{nmq}-\psi_{nmr})\sinh\xi_{nmq}\sinh\xi_{nmr}\cosh\xi_{nms}]$$

$$G_{nmp} = \frac{(-1)^{p-1}}{2\Delta_{nm}} [\xi_{nmq}(\psi_{nmr}-\psi_{nms})\cosh\xi_{nmq}\sinh\xi_{nmr}\sinh\xi_{nms}$$
$$+ \xi_{nmr}(\psi_{nms}-\psi_{nmq})\sinh\xi_{nmq}\cosh\xi_{nmr}\sinh\xi_{nms}$$
$$+ \xi_{nms}(\psi_{nmq}-\psi_{nmr})\sinh\xi_{nmq}\sinh\xi_{nmr}\cosh\xi_{nms}]$$

$$P_{nmp} = \frac{(-1)^{v-1}}{2\Delta_{nm}} [(\phi_{nmr}\xi_{nms}-\phi_{nms}\xi_{nmr})\sinh\xi_{nmq}\cosh\xi_{nmr}\cosh\xi_{nms}$$
$$+ (\phi_{nms}\xi_{nmq}-\phi_{nmq}\xi_{nms})\cosh\xi_{nmq}\sinh\xi_{nmr}\cosh\xi_{nms}$$
$$+ (\phi_{nmq}\xi_{nmr}-\phi_{nmr}\xi_{nmq})\cosh\xi_{nmq}\cosh\xi_{nmr}\sinh\xi_{nms}]$$

Suffixes $p$, $q$, $r$ and $s$ are recurring numbers of 1, 2, 3, and 4 and $q$, $r$ and $s$ are the three numbers except $p$ arranged in the numerical order. Let the formula obtained by interchanging *sinh* and *cosh* in $\Delta_{nm}$ be $\Delta_{nm}'$. $A_{nmp}'$, $C_{nmp}'$, $G_{nmv}'$ and $P_{nmp}'$ are obtained by interchanging *sinh* and *cosh* and taking $\Delta_{nm}'$ in place of $\Delta_{nm}$ in the formulas of $A_{nmp}$, $C_{nmv}$, $G_{nmv}$ and $P_{nmp}$ respectively.

## References


(1) R. N Arnold and G.B. Warburton : Proc. Inst. Mech. Engr., Lond., Vol. 167 (1953), p. 62.

(2) G. B. Warburton : J. Mech. Engng. Sci., 7—4(1965), p. 399.

(3) G. B. Warburton & A. M. J. Al-Najafi : J. Sound & Vibration, 9—3(1969), p. 373.

(4) S. Takahashi et al. : Bulletin of the JSME, Vol. 13, No.61 (1970), p. 850.

(5) S. Timoshenko, S. Woinowsky-Krieger : Theory of Plates and Shells, 2nd. ed. Mcgraw-Hill, (1959).

(6) S. Takahashi : Bulletin of the JSME, Vol. 12, No. 49 (1969), p. 43.

山形大学紀要（工学）第12巻　第1号　昭和47年1月

# 複合円筒の振動について

## （変位，曲げモーメント，せん断力）

鈴木勝義・高橋　伸・平野芳太郎

山形大学工学部機械工学科

二個の半径が等しく厚さは異なる円筒を縦につないだ系（複合円筒）の振動数を著者らは前に求めたが，続いて本論文では複合円筒の変位，曲げモーメント，せん断力の分布を調べた。複合円筒は，両端固定または厚い方の円筒の一端を固定，薄い方の円筒の一端は自由としている。この種の問題は大型の液体容器（石油タンクなど）や煙突の振動にみられる。数値計算は周方向の波の数($n$)が3の場合の変位，まげモーメント，せん断力を求めまた，同じ振動数で厚さが複合円筒の厚い方の円筒に等しい単一円筒と比較した。